Possibility of the presence of S, SO_2, and CO_2 at the poles of the Moon

Alexey A. Berezhnoy*, Nobuyuki Hasebe, Takuji Hiramoto

Advanced Institute for Science and Engineering, Waseda University, 3-4-1 Okubo, Shinjuku-ku，Tokyo 169-0071

* *Also at Sternberg Astronomical Institute, Moscow State University, Moscow, Russia*

Email (AB) iac02074@kurenai.waseda.jp

and

Boris A. Klumov

Institute of Dynamics of Geospheres, Moscow, Russia

(Received 2003 March 4)

Abstract

The presence of volatiles near lunar poles is studied. The chemical composition of a lunar atmosphere temporarily produced by comet impact is studied during day and night. C-rich and long-period comets are insufficient sources of water ice on the Moon. O-rich short-period comets deliver significant amounts of H_2O, CO_2, SO_2, and S to the Moon. An observable amount of polar hydrogen can be delivered to the Moon by single impact of O-rich short-period comet with diameter of 5 km in the form of water ice. The areas where CO_2 and SO_2 ices are stable against the thermal sublimation are

estimated as 300 and 1500 km^2, respectively. If water ice exists in the 2 cm top regolith layer CO_2 and SO_2 ices can be stable in the coldest parts of permanently shaded craters. The delivery rate of elemental sulfur near the poles is estimated as 10^6 g/year. The sulfur content is estimated to be as high as 1 wt % in polar regions. The SELENE gamma-ray spectrometer can detect sulfur polar caps on the Moon if the sulfur content is higher than 1 wt %. This instrument can check the presence of hydrogen and minerals with unusual chemical composition at the lunar poles.

Key words: Moon, astrochemistry, molecular processes, comets: general, gamma rays: theory

1. Introduction

The possible existence of water ice in permanently shadowed regions near the lunar poles was postulated by Watson et al. (1961). Arnold (1979) investigated the delivery rate of water into the cold lunar polar craters due to degassing from the lunar interior, micrometeorite bombardment, solar wind, and comet impacts. Modeling of the Moon's obliquity over time indicates that polar terrains have harbored permanent shade for 2-3 billion years, exposing them to a host of potential sources of volatiles.

Some experiments have been made to search for the existence of water in the polar

regions. Ice-like radar echoes were detected there by the Clementine-Deep Space Network bistatic experiment (Nozette et al. 1996, 2001). Another attempt to detect hydrogen-containing compounds near the lunar poles was made using Lunar Prospector neutron data (Feldman et al. 1998). Feldman et al. (2000) estimated the mass of water ice as $2*10^{14}$ g in the South pole region, and its mass fraction as about 1.5 % in the south polar caps. The observable amount of lunar polar hydrogen can also be explained by the action of permanent solar wind flux on the lunar surface (Starukhina, Shkuratov 2000). This origin of lunar polar hydrogen is preferable to the comet hypothesis because a geological period of time is not required for the survival of lunar volatiles in the polar caps. However, a recent analysis of hydrogen content based on Lunar Prospector data supports the idea that a significant portion of the enhanced hydrogen near the poles is most likely in the form of water molecules (Feldman et al. 2001).

The possibility of polar volatiles other than water ice has been considered by Sprague et al. (1995), Butler (1997), and Duxbury et al. (2001). Sprague et al. (1995) proposed that the unusual radar properties of the Hermean poles make a compelling case for the presence of elemental sulfur in the upper layers of the polar regolith on Mercury. The thermal stability of sulfur near the lunar poles was considered by Vasavada et al. (1999). But the sulfur delivery rate and the possible existence of SO_2 ice on the Moon have not been considered so far.

The comet hypothesis for the origin of lunar polar volatiles has not been well studied. The fraction of cometary matter captured by the lunar gravitation field was estimated by Klumov and Berezhnoi (2002), which showed that volatile compounds in the temporary lunar atmosphere were accumulated completely in cold traps. Water is thought to be delivered episodically to the cold traps near the lunar poles through low-speed collisions of big comets with diameter D > 5 km (Berezhnoi, Klumov 1998; Berezhnoi, Klumov 2000). The lunar atmosphere temporarily formed by an impacting comet is not dense enough to account for the neutron data obtained by Lunar Prospector, if the comet size is less than 5 km. Such an atmosphere cannot predict sufficient water molecules from photolysis by UV solar radiation. Berezhnoi and Klumov (2000) considered the chemical composition of the lunar atmosphere formed by the comet collision, though the thermal stability of lunar volatiles in cold traps, the condensation of volatiles on the night side of the Moon, and their adsorption by lunar regolith were not studied.

In this paper, we estimate the possibility of collisions of large comets with the Moon and consider the existence of CO_2 and SO_2 near the poles. It is aimed at studying on the presence of elemental sulfur at the poles. We also discuss the possibility of detection of sulfur and hydrogen in the polar regions by gamma-ray spectroscopy.

2. Cometary origin of lunar volatiles

We consider the cometary origin of lunar polar hydrogen. On comet impact the following processes occur: vaporization of cometary matter, vaporization, melting, and fragmentation of the regolith, ejection of multiphase cometary matter and lunar soil, and the formation of an impact crater. After the comet impact the Moon captures a part of the cometary matter. As numerical and analytical estimates show, the velocity distribution along the radius r in the fireball is close to linear $V(r) \sim V_{max}\ r / R_{max}$, where V_{max} is the velocity of the outer cloud edge, R_{max} is the radius of edge (Zel'dovich, Raizer 1967). $V_{max} = c(v)\ V_i$, where V_i is the impact velocity of the comet. At impact velocities of 10-20 km/s, c(v) = 0.3-0.5. If we neglect the dependence of density on the radius, the part of fireball matter captured by the lunar gravitational field can be estimated as $(V_{esc}/ V_{max})^3$, where V_{esc} = 2.4 km/s is the escape velocity from the Moon. For high-speed impacts with V_i > 30 km/s the mass of impact vapor increases as V_i^2 with increasing velocity (Ahrens, O'Keefe 1977), then $c(v) \sim V_i^{-2}$ and V_{max} = const. The total amount of captured materials decreases with increasing impact velocity at V_i < 30 km/s. Assuming that c(v) = 0.3 at V_i < 30 km/s and $C(v) = C(30\ km/s)(30\ km/s/V_i)^2$ at V_i > 30 km/s the mass-fraction of vapor cloud induced by impact and captured by the Moon is 0.06, 0.01, and 0.01 at impact velocities equal to 20, 30, and 60 km/s, respectively. Similar results can be obtained based on the model of Moses et al.

(1999). The mass-fraction of the impact-induced vapor cloud retained by the Moon is estimated to be 0.2, 0.03, 0.01, and 0.003 at impact velocities equal to 20, 30, 40, and 60 km/s, respectively.

Let us check the probability of comet impacts. According to the analysis of orbital evolution of known short-period comets, the total impact probability is about $2*10^{-8}$ $year^{-1}$ for comets with D > 0.4 km and a mean speed of collisions, 18 km/s (Jeffers et al. 2001). Impact probabilities and mean impact velocities are equal to $9*10^{-9}$ $year^{-1}$ and 58 km/s for Halley-type comets, and $2*10^{-8}$ $year^{-1}$ and 52 km/s for long-period ones. Since the probability of low-speed collisions is maximal for short-period comets, most of the volatiles seem to be delivered to the Moon by these comets. Using the size distribution of short-period comets $N (> D) \sim D^{-2.07}$ (Donnison 1986), we can estimate that there should be one collision of a 3-km comet and 10 collisions of 1-km comets with the Moon over last three billion years. However, the discovery of short-period Earth-crossing comets is not complete because extinct comets are much more difficult to observe than active ones. Shoemaker et al. (1994) believe that the extinct/active ratio for short-period comets is ~18. If we take the number of non-active short-period comets into consideration 10-20 times more than that of active comets, the biggest short-period comet to have collided with the Moon has a diameter of about 10 km. Note that almost all volatiles of cometary origin were delivered to the Moon by a few large comets

because the spectral index of the comet size distribution is less than 3.

At the time of collision of asteroids and comets with the Moon, the temperature and pressure in the impact-formed fireball can reach 10^4 K and 10^3 bars, respectively. At the beginning of fireball expansion, the gases are in thermodynamic equilibrium because the hydrodynamic time scale is much shorter than time scale of chemical reactions. As the fireball expands and cools adiabatically, the rate of chemical reactions drops and the time scale of chemical processes increases. When the hydrodynamic and chemical time scales become comparable, quenching process dominates and virtually no further changes take place in relative abundances of species. The hydrodynamic time scale t_{hd} is $t_{hd} \sim R/c_s \sim 1$ s, where R ~ 1 km is the impactor diameter, and $c_s \sim 1$ km/s is the sound speed at 2000 K. The time scale of chemical processes

$$t_{chem} \sim ([X]*k)^{-1}, \qquad (1)$$

where [X] is the abundance of reactive molecule, and k is the reaction rate constant. The major reactions occurring in fireball are given by reactions (A-C) have high values of activation energy. Quenching of reaction (B) occurs for 2000 K at 10^{-6} bars, but for 1000 K at 10^{-3} bars. Reactions with lower activation energy have lower quenching temperature and pressure.

$H + H_2O = H_2 + OH$ (A), $1.6*10^{-11} (T/300)^{1.2} \exp(-9610/T)$ cm^3/mol.*s

$H + CO_2 = OH + CO$ (B), $3.38*10^{-10} \exp(-13160/T)$ cm^3/mol.*s

$H_2 + CO_2 = H_2O + CO$ (C), $2.9*10^{-14} (T/300)^{0.5} \exp(-7550/T)$ $cm^3/mol.*s$

The chemical composition of the fireball after the quenching moment depends on the quenching parameters and the elemental composition of the fireball. According to spectroscopic observations most comets have an O/C ratio greater than unity. In this case at P_{quench} ~ 0.01 –10 bars and T_{quench} ~ 2000 K, the major components of a fireball are H_2O, H_2, CO, but at T_{quench} ~ 500-700 K they are H_2O, H_2, CO_2 and CH_4 (Klumov, Berezhnoi 2002). The chemical composition of the fireball can be quenched at low temperatures, if catalysis of chemical reactions is very effective on the surface of silicate grains formed during fireball expansion. So water is the main component of the fireball for a wide range of P_{quench} and T_{quench}. The water content, however, is low if O/C < 1 in the impactor matter. These environmental conditions can be realized for collisions of some asteroids and C-rich comets with high dust/ice ratios (see figure 1). Then water can enter the composition of the impact-produced atmosphere, if O/C > 1 in the comet. As we show later, the exact determination of quenching temperature and pressure in fireball is not important because photochemical processes and the elemental composition of the cometary nucleus determine the chemical composition of the impact-produced lunar atmosphere.

Let us consider the question about content of sulfur-containing compounds in the fireball. When fireball is cooling below 1500 K, H_2S becomes the main S-containing

compound. The reaction rate constant of sulfur fixing into solid phase is given by

$$dFe/dt = k_f P(H_2S) - k_r P(H_2), \qquad (2)$$

where k_f = 5.6exp(-27950/RT) cm/hour*bar, k_r = 10.3exp(-92610/RT) cm/hour*bar (Lauretta et al. 1996). At $[H_2S]/[H_2]$ ~ 0.01, the back reaction is faster at T > 1500 K. The time t_{chem} required for sulfidisation of Fe grains can be estimated as $t_{chem} \sim r(Fe) / k_f P(H_2S)$ (3), where $r(Fe) \sim 10^{-3}$ cm is a typical radius of Fe grains. Therefore, the hydrodynamic and chemical time scales at 1000-1500 K are comparable at $P(H_2S) \sim 1$ bar or at a total pressure of about 300 bars. But such high values of the pressure are typical for the beginning of fireball expansion, when T >> 1500 K. This means that sulfur fixation into the solid phase is kinetically inhibited and sulfur-containing species migrate into the lunar atmosphere.

We assume that the gases remaining on the Moon after comet impact expand with the speed of sound because the remaining gases expand into vacuum. Then the formation period of lunar atmosphere can be estimated as $D/c_s \sim 2*10^4$ s, where D = 3476 km is the diameter of the Moon, and $c_s \sim 0.3$ km/s is the sound speed at 300 K. So, this period of time is much shorter than the photolysis time scale (10^5 - 10^6 s). The period for condensable gases to be captured by cold traps is shorter than the period for the atmosphere to be lost by exposure to UV solar photons, but both times are proportional to the mass of the temporary atmosphere (Klumov, Berezhnoi 2002). For

example water molecules in an impact-produced atmosphere with an initial number density of 10^{14} cm^{-3} can be captured by cold traps in 10^{10} s and be lost due to photolysis in 10^{11} s. Therefore, the capture probability of volatiles from an impact-produced temporary atmosphere by cold traps is about unity and independent of the impact place and initial number density. However, the capture probability of volatiles increases with the latitude at the impact site of micrometeoroids (Crider, Vondrak 2000). The period for gases to be captured by cold traps is estimated based on the intensity of diffusion of gases in the temporary atmosphere. The diffusion mechanism of capture of gases is valid in a collisionally thick atmosphere. The maximal number density in a collisionless lunar exosphere at 300 K is about 10^{8} cm^{-3}, it corresponds to an atmospheric mass of $5*10^{9}$ g (Vondrak 1974). About 10 % of cometary matter is retained on the Moon for collisions with a low speed comet (Berezhnoi, Klumov 1998). Then comets over 10^{11} g can produce a thick atmosphere. Gases remaining as a lunar atmosphere are chemisorbed by the lunar regolith. Let us estimate the maximal mass of adsorbed water. If 10 layers of molecules are chemisorbed on the surface with mean area per molecule of 10^{-15} cm^{-2}, about 10^{11} g of cometary gases can be bound on the surface of the Moon. Adsorption can also take place in subsurface layers due to transport of water molecules in the regolith. The typical content of adsorbed water in the lunar regolith may reach 1000 ppm (Cocks et al. 2002). If the water content in the upper 0.1 mm regolith layer

reaches 1000 ppm after comet impact then 10^{13} g of water can be bound on the surface at a regolith density of 2 g/cm^3. The rate of adsorption estimated by (Hodges 2002) is higher than the photolysis time scale (10^5 s). This means that almost all water molecules of cometary origin are bound by the regolith in the equatorial regions and the capture probability of water by cold traps is low, if the mass of water in the impact-produced atmosphere is less than 10^{13} g.

Photochemical processes in the temporary atmosphere determine the chemical composition of volatiles in cold traps because the duration of capture of volatiles is greater than the photolysis time scale. The photochemical model was described in a previous article (Berezhnoi, Klumov 2000), where the initial chemical composition of the atmosphere was considered. Namely, at the moment of formation of the atmosphere, H_2, H_2O, CO, and CO_2 are the major components. This case is realized when T_{quench} ~ 1000 – 2000 K, P_{quench} ~ 0.01 – 1 bar and at O/C >1 in cometary matter. Rate constants of neutral-neutral reactions were taken from references (Baulch et al. 1976; Nimmo et al. 1998; Le Teuff et al. 2000), and the rates of photo processes at 1 AU for a quiet Sun were taken from Huebner et al. (1992). Molecules are destroyed by solar photons and are formed mainly through three-body reactions. Photo rates are assumed to be independent from the number density at the surface. The set of reactions does not include ion-neutral reactions and chemical processes on the lunar surface. However the

chemical composition of the fireball in the equilibrium at T~ 1000-2000 K and P~ 10^{-3} – 10 bar, determined by the photochemical program, is similar to that determined by thermodynamic calculations. This means that the set of major reactions is complete and the reaction rates used are correct.

The period of a temporary atmosphere captured by cold traps (10^{10} s) is much larger than the duration of the lunar day ($3*10^{6}$ s). Therefore, the photochemical model was modified, including the dependence of photo rates on time. It is assumed that comet impacts occur at sunrise. We adopted comet Halley's composition (H- 48.4, O- 30.4, C- 13.7, N- 2.3, Si- 1.6, Mg- 1.1, Fe- 1.1, S- 1; these values represent the number of atoms) for an O-rich comet with almost equal masses of dust and gas components in cometary matter (Delsemme 1991), and the following composition (H- 18.4, O- 15.4, C- 13.7, N- 2.3, Si- 1.6, Mg- 1.1, Fe- 1.1, S- 1) for a C-rich comet. Dust has C/O > 1, gas has C/O < 1 in comet Halley. So an increasing dust/gas ratio leads to an increasing C/O ratio in a comet. Thermodynamic calculations show that the addition of lunar soil to the fireball does not change the chemical composition of volatiles in the impact vapor because the content of volatiles in lunar soil is very low in comparison with comets. From this reason we assumed that the fireball only consists of cometary matter.

The main reactions determining the daytime water content in the temporary atmosphere are

$H_2O + h\nu = OH + H$ (D), $10^{-5}\ s^{-1}$

$OH + H + M = H_2O + M$ (E), $6*10^{-26}\ T^{-2}\ cm^6/mol.^2*s$

$OH + H_2 = H_2O + H$ (F), $1.55*10^{-12}\ (T/300)^{1.6}\ \exp(-1660/T)\ cm^3/mol.*s$

$OH + CO = CO_2 + H$ (G), $1.7*10^{-13}\ (T/300)^{0.95}\ \exp(74/T)\ cm^3/mol.*s$

$H_2 + h\nu = H + H$ (H), $8.2*10^{-8}\ s^{-1}$

$H + H + M = H_2 + M$ (I), $3*10^{-30}/T\ cm^6/mol.^2*s$.

Reaction (E) at low number densities is slower than reaction (G). Reaction (F) is slower than reaction (G) at T < 500 K. This means that due to the photolysis of water H_2O and CO molecules are converted into CO_2, H, and H_2. The rate of reaction (E) increases faster than that of reaction (D) with increasing number density; this leads to an increasing quasi-equilibrium daytime water content with increasing number density.

Now we will consider a low quenching temperature for the collisions of C-rich comets. After a collision of a C-rich comet, the major components of the fireball are H_2 and CO (see figure 1). The results of kinetic calculations are presented on figure 2. The composition of the temporary atmosphere in quasi-equilibrium is reached 10^7 s after the moment of impact. The abundances of atoms in the daytime are higher than those at nighttime. The H_2O and CO_2 contents in the atmosphere are very low. Then water cannot be delivered to cold traps by impacts of C-rich comets. However, S, SO_2, and HCN abundances in the temporary atmosphere formed by such comets' impact are

high. It means that these species are delivered to the lunar poles by C-rich comets.

After impact of an O-rich comet, major species in the fireball after stopping of chemical processes are H_2, H_2O, CO, and CO_2 (see figure 1). When the total number density is the same the chemical composition of the atmosphere formed by O-rich comets is quite different in comparison with impacts of C-rich comets (see figure 3). The water and carbon dioxide content in the temporary atmosphere are 5-7 orders of magnitude higher than those of impacts of C-rich comets. H_2S is the main sulfur-containing component of the fireball. In the temporary atmosphere, H_2S molecules are transformed into S and SO_2. The same behavior occurs for NH_3 and CH_4. These compounds are easily destroyed by solar photons. The atmospheric composition in quasi-equilibrium formed by O-rich comets is very similar at high and low quenching temperatures of chemical processes in the fireball (see figures 3, 4). Then the influence of quenching parameters is weak on the composition of an impact-produced atmosphere. This means that the chemical composition, including volatiles captured by cold traps, is determined by the impact velocity, the mass of the impacting comet, and the O/C ratio in the impactor.

The daytime concentration of H_2O, CO_2, and SO_2 rapidly increases with increasing total number density. The nighttime concentration of condensable gases shows a slow increases with the increase of number density. However, in these calculations, the

possible condensation of water on the night side of the Moon was not considered. The nighttime temperature on the Moon is low enough for condensation of water and SO_2, but not for condensation of CO_2. So the movement of SO_2 and H_2O molecules toward the poles occurs only on the day side. The daytime water content is less than 1 % at total number densities < 10^{13} cm^{-3} and 1-3 % at densities > 10^{13} cm^{-3} (see figure 4). The number density 10^{13} cm^{-3} corresponds to a mass of atmosphere of $5*10^{14}$ g when a short-period comet with a mass of about $3*10^{15}$ g impacts. The observable amount of water ice ($2*10^{14}$ g) at the south pole (Feldman et al. 2001) was possibly delivered to the Moon by a single impact of a 5-km short-period comet. CO_2 ices can be formed by impacts of big comets as well by impacts of small comets, because the motion of CO_2 molecules toward the poles occurs on both sides of the Moon.

3. Thermal stability of SO_2 and CO_2 ices at the poles of the Moon

Comets are important sources of lunar polar volatiles. For example the impact of a O-rich low-speed comet with diameter of 5 km creates a temporary atmosphere with a number density of 10^{14} cm^{-3} on the Moon. Transferring abundances of condensable gases (see figure 4) to their masses we can estimate that such impact can deliver to the polar caps about $3*10^{14}$ g of water ice, $3*10^{15}$ g of CO_2 ice, $5*10^{14}$ g of SO_2 ice, and $3*10^{13}$ g of elemental sulfur. Other volatiles like NH_3, HCN, H_2S, PH_3, H_2CO, and

CH_4 could be delivered to the lunar polar caps, while their abundances are very low in oxidant lunar atmosphere formed by comet impact.

Let us consider the survival of volatile compounds delivered to the lunar poles by comet impacts. Crider and Vondrak (2000) show that a slow steady source like the solar wind has provided enough hydrogen over 80 Myr to account for the observed deposits. This means that more than 95 % hydrogen delivered to the Moon by steady sources is lost from the cold traps. After a 5-km short-period comet impact, a 30 cm ice layer is formed at the lunar polar caps over an area of 10^4 km^2. A 30 cm CO_2 ice layer evaporates over $3*10^5$ years at 70 K, and over 300 years at 80 K (Vasavada et al. 1999). The depth of less volatile water ice is only 3 cm. Micrometeorite bombardment, Lyman alpha radiation, and cosmic ray sputtering can destroy an ice layer at the surface (Lanzerotti et al. 1981). Using the model of (Killen et al. 1997) and the value of the micrometeoroid flux on the Moon from (Morgan, Shemansky 1991), a 3 cm water ice layer can be destroyed by micrometeorite bombardment and other energetic processes at the surface at 90 K over 100 Myr. The gardening effect of regolith due to micrometeorite bombardment, which plays an important role in regolith processes, leads to the preferential survival of buried ice deposits. For example the sublimation rate of ice under 1 cm of dust is 100 times less than that of ice at the surface (Killen et al. 1997). Let us assume that subsurface ice is stable at a depth deeper than 1 cm.

According to Apollo data, a regolith layer down to D_m = 1 cm in depth is mixed over a period of $t_m = 10^6$ years by the gardening effect of micrometeorite processes, and $D_m \sim t_m^{1.5}$ (Neukum, Ivanov 1994). Comparing rates of burial and the loss rate due to micrometeorite bombardment we can state that only water ice layers with a depth less than 1 mm cannot be buried due to the high intensity of surface loss processes. So the sublimation rate must be less than 1 mm per million years for the formation of burial ice deposits. When temperatures are lower than 59 K for CO_2, 78 K for SO_2, 112 K for H_2O ices, and 218 K for sulfur deposits (Vasavada et al. 1999), polar ice exposed becomes stable. As the vapor pressure of volatiles is expressed by an exponential function of temperature, the sublimation loss rate is controlled by maximal surface temperature. Let us estimate the area at the lunar poles where ices would be retained for 10^6 years, because of the reduced sublimation rate of their molecules at low temperature. The maximal temperature at the coldest surface is less than 60 K only for craters Amundsen, Nansen, Hermite, and U. The total area where CO_2 ice at the surface is thermally stable is about 300 km^2 (see figures 11, 12 of Vasavada et al. (1999)). The maximal surface temperature is less than 80 K for the cold regions of craters Amundsen, Nansen, Hermite, Shackleton, T, U, and V (see figure 11 of Vasavada et al. (1999)). The total area where SO_2 ice is stable can be estimated as 800 km^2 at south and 700 km^2 at north.

If a regolith layer covers an ice layer, the ice would be protected from surface loss processes. Then the loss rate through the upper regolith layer could be limited by a reduced coefficient of diffusion. Let us study the temperature regime in the polar caps. The temperature at a given depth is determined by the mean surface temperature and the thermal gradient. The thermal gradient is given

$$dT/dz = -Q/k \qquad (3).$$

where Q is the heat flow out of the lunar interior and k is the thermal conductivity. The heat flow is equal to $2.2*10^{-6}$ W/cm^2 at the Apollo 17 landing site (Langseth et al. 1976).

The thermal conductivity depends on the particle size, bulk density, temperature, and the presence of volatiles. According to (Langseth et al. 1976), the top 1-2 cm lunar regolith has an extremely low thermal conductivity ($1.5*10^{-5}$ W/cm*K), and the conductivity becomes as large as 5-7 times greater at a depth of 2 cm. At the Apollo sites, the mean temperatures at 35 cm below the surface are 40-45 K. In addition, a small amount of water ice can significantly increases the thermal conductivity in the top 2 cm regolith layer. Recent studies of the temperature regime for polar lunar craters (Vasavada et al. 1999; Hale, Hapke 2002) unfortunately do not include the dependence of heat conductivity on water ice abundance in the regolith. We have used the model proposed by Mellon et al. (1997) to estimate the thermal conductivity of mixtures of

lunar regolith and water ice. The thermal conductivity of water ice is 4.9/T + 0.005 W/cm*K for temperatures between 108 and 273 K (Hobbs 1974). Due to a big difference of thermal conductivity between dry regolith and water ice, the inclusion of even 0.01 wt % water ice to the dry regolith leads to a disappearance of the temperature difference between the surface and the depth of 1-2 cm (see figure 5).

The sublimation rate of ice from the subsurface can be estimated using the model by Fanale and Salvail (1989). Based on this model subsurface, pure CO_2, SO_2, and H_2O ices at 2 cm depth are stable at mean temperatures less than 80, 110 and 140 K, respectively. If there is water ice down to 2 cm depth in the regolith, a difference of regolith temperature between surface and subsurface is absent. Then buried CO_2 ice is stable at a mean surface temperature of less than 80 K and buried SO_2 ice is stable at a mean surface temperature of less than 110 K. These restrictions on the temperature are not so strong as the restrictions for the stability of surface CO_2 and SO_2 ices. This means that buried ices are stable for geological periods of time.

If the top 2 cm regolith layer in polar regions is covered by soil with extremely low heat conductivity as in the equatorial region, the difference between average temperatures at the surface and 30 cm in depths can reach 40 K. The stability of CO_2 and SO_2 ices at subsurface requires mean diurnal surface temperatures less than 40 and 65 K, respectively. Therefore, CO_2 subsurface ice is unstable, while SO_2 ice is stable

only in the coldest part of lunar polar craters Amundsen, Nansen, Hermite, T, U, and V (see figure 12 in reference (Vasavada et al. 1999)).

However, CO_2 and SO_2 molecules can be chemisorbed by fine dust particles in the surface. The mobility of adsorbed molecules in those regions is not so high as that of ice. A recent study (Cocks et al. 2002) shows that adsorbed water is kinetically stable even at 255 K in comparison with the stability of crystalline water ice only at $T < 110$ K. The adsorption capacity of lunar soils is about 0.1 wt % (Cocks et al. 2002). The same behavior is expected for SO_2 and CO_2 molecules. Then adsorbed SO_2 and CO_2 molecules lower than 0.1 wt % can exist near the lunar poles at temperatures of about 200 K.

Next we assume that comets are the major source of lunar polar volatiles and that the relative abundances of H_2O, SO_2, and CO_2 ices in regions where they are thermally stable are the same as in a temporary atmosphere with number density of 10^{13} cm^{-3} of cometary origin (see figure 3). Then the CO_2 and SO_2 contents in such regions are 10 and 2 wt %, respectively, together with 1.5 wt % water ice (Feldman et al. 2000). Those values are an upper limit for CO_2 and SO_2 abundances at the poles of the Moon. If comets are not the major source of lunar volatiles, the average abundances of CO_2 and SO_2 will be much smaller. The upper limit of area with CO_2 and SO_2 thermal stability is 300 km^2 and ~ 1500 km^2, respectively. If there is a temperature difference between

polar subsurface and surface like that in equatorial regions, the area thermally stable for these ices will be much smaller.

4. Sulfur at the poles of the Moon

Lunar materials rich in sulfur may be used as important resources in the near future (Vaniman et al. 1992). In Apollo returned samples, the sulfur abundance in the form of FeS varies from 0.05 to 0.3 wt % (Moore et al. 1974). The sulfur content at the lunar poles would be higher than that in the equatorial region because sulfur is a volatile element. Let us estimate the delivery rate of elemental sulfur to the lunar poles. The sulfur on the Moon is delivered through asteroid and comet impacts, solar wind, and micrometeorite bombardment.

Comet impacts are important sulfur sources. If a comet produces a temporary atmosphere with a number density less than $5*10^{12}$ cm^{-3}, the main sulfur-containing compounds in this atmosphere would be atomic sulfur (see figure 4). This value of number density can be reached during collisions of 2-km short-period comets with the Moon. Performing similar calculations for the case of 5-km comets, about $3*10^{14}$ g of sulfur is estimated to be delivered to the polar traps by non-active comet impacts.

The mass of sulfur of asteroid origin captured by lunar poles can be estimated as $M \sim f_1*f_2*f_3*f_4*N*M_{ast}$, where f_1 is the probability of trapping sulfur atoms from the

lunar atmosphere by cold traps, f_2 is the fraction of asteroid mass captured by the lunar gravitational field, f_3 is the ratio between the mass of sulfur released into a lunar transient atmosphere to the total mass of sulfur in an asteroid, f_4 is the mean sulfur abundance in asteroids, N is number of collisions during the last three billion years, and M_{ast} is the mean mass of colliding asteroids.

Werner et al. (2002) estimated that there were about 700 collisions of asteroids with D > 1 km with the Moon over the last $3*10^9$ years. Taking account of the size distribution function for asteroids (Rabinowitz et al. 1994), we can estimate that $N*M_{ast} \sim 10^{19}$ g at the mean density of asteroids of 3 g/cm^3. We analyze the collisions between asteroids and the Moon based on the model of comet impacts described in section 2. We also assume that sulfur, carbon and water abundances in asteroids are 1 wt %, 1 wt %, and 0.3 wt %, respectively. It is assumed that $f_3 \sim 0.3$. The depletion of sulfur content in Apollo samples confirms the sulfur release from the regolith into the lunar atmosphere during impact events. CO, H_2, and S remain in the transient lunar atmosphere after an asteroid impact. The CO_2 and H_2O content in such an atmosphere is low, because the amount of carbon in most asteroids exceeds the amount of oxygen not bound by metals. When typical collision velocity between the asteroid and the Moon is 15-20 km/s (Jeffers et al., 2001), f_2 is equal to 0.1 (see section 2). The chemical composition of the lunar atmosphere of asteroidal origin depends on the impact velocity, and the chemical

composition of the impactor and lunar soil. Impacts of 1 km and 5 km asteroids lead to the formation of a transient atmosphere with the number densities of $5*10^9$ and $5*10^{11}$ cm^{-3} near the surface, respectively. So asteroid impacts create a thick lunar atmosphere, if we neglect chemisorption of molecules on the surface. Due to the high efficiency of the diffusion mechanism of trapping of condensable species, the factor f_1 is about unity (see section 2 for more details). Then the total mass of sulfur of asteroidal origin is estimated to be 10^{15} g. The probability of CO_2, H_2O, and SO_2 trapping by cold traps is low, because a thick transient atmosphere cannot protect complex molecules from photolysis by UV solar photons.

In the following, we estimate the capture probability K of volatile compounds delivered to the Moon by micrometeorite bombardment. Using a simple ballistic model, the value of K can be estimated at $K << 1$ as

$$K \sim c\, t_{ph}\, S_{tr} / t_{mig}\, S_m \qquad (4)$$

$$t_{mig} = 2/a\, (RT/M_r)^{0.5} \qquad (5),$$

where $c \sim 1$ is the capture probability of molecules during their collisions with the surface of cold traps, t_{ph} the typical photolysis time taken from Huebner et al. (1992), S_{tr} the area of cold traps, t_{mig} the mean duration of hops, and $S_m = 3.8*10^7$ km^2 the total area of the lunar surface. We take $a = 1.62$ m/s^2 for the surface gravity on the Moon, R the universal gas constant, and M_r the molecular mass of a volatile compound.

The area of permanently shaded regions on the Moon is about 8000 km^2 (Margot et al. 1999), this value is used as the area of water ice stability. Vasavada et al. (1999) estimated the latitudes of regions where sulfur is stable against thermal sublimation between 86-90 degrees, which corresponds to an area of about 10^5 km^2. Based on estimates made in section 3, we assume that the area of cold traps for SO_2, H_2S, and CO_2 molecules are equal to 1500, 300, and 300 km^2, respectively (the volatility of H_2S molecules is similar to that of CO_2 molecules). The calculation results at 300 K based on formulae (4) and (5) are shown in table 1.

As can be seen from table 1, the capture probability of SO_2 and H_2S molecules is very low due to their small area of thermal stability and short photolysis times. The capture probabilities of H_2O and CO_2 are similar to those obtained by Monte Carlo simulations (Butler, 1997). However, the validity of ballistic motion of water molecules on the lunar surface was ruled out by Hodges (2002a). Butler (1997) shows that the ballistic mechanism is not valid for the motion of sulfur atoms on the Mercurian surface. The ballistic model is based on thermal desorbtion of molecules from the lunar surface. If molecules chemisorb on the surface, they can be desorbed only during meteoroid impacts. In this case for ”high” temperature molecules in the exosphere, the capture probability decreases as $K \sim T^{-0.5}$ with increasing temperature, if photoionisation is dominant in the escape mechanism. However, the average velocity of sulfur atoms at

2000-3000 K is comparable with the escape velocity from the Moon. Therefore, Jeans escape is more efficient than escape caused by photoionisation. Let us use $f_1 = 0.1$ as a realistic value for sulfur. Detailed experimental investigations of sulfur adsorption are required for better understanding of sulfur transport on the Moon. When sulfur is detected in the lunar exosphere, and the velocity and number density of sulfur atoms is determined, then more detailed model of behavior of sulfur atoms on the Moon would be proposed.

Based on measurements of terrestrial cosmic dust flux (Love, Brownlee 1993), the micrometeorite flux on the Moon is about $2*10^9$ g/year. The mean impact velocity of incoming meteoroids is 15.8 km/s (Morgan, Shemansky 1991). The parameter f_2 can be estimated using a Maxwellian velocity distribution function. A significant fraction of the sulfur atoms remain on the Moon, if the initial temperature is less than 8000 K during impact events. The parameter f_3 is similar to those for asteroid and micrometeoroid impacts, because the collision velocities of asteroids and micrometeorites are comparable. Assuming that parameters f_2, f_3, and f_4 are the same as for asteroid impacts, about $3*10^{14}$ g of sulfur originating from micrometeorites is estimated to have been captured by cold traps over the last three billion years.

The solar wind flux at 1 AU is $4*10^8$ $cm^{-2}s^{-1}$. The S/H ratio in the solar wind is equal to $2*10^{-5}$ (Shafer et al. 1993). Sulfur atoms are implanted in the regolith by the

solar wind, and they are delivered to the lunar exosphere by impact events. Assuming that 1 % of implanted sulfur atoms are captured by cold traps, it is estimated that about 10^{14} g of sulfur of solar wind origin could have been delivered to lunar cold traps over the last three billion years.

So sulfur delivery attributed to asteroid and comet impacts, solar wind, and micrometeorite bombardment, are comparable to each other. About $2*10^{15}$ g of sulfur in total has been delivered to cold traps. Though the loss mechanisms, their rates and the delivery rate of sulfur at the lunar poles are not clear, the loss rate of sulfur is less than that of water due to a lower partial pressure, higher atomic mass and longer photo destruction time. If we neglect the loss mechanisms of sulfur from cold traps, we can estimate the sulfur content to be as high as 2 g/cm^2 in regions of sulfur stability with an area of 10^5 km^2. During the existence of current cold traps (2-3 billion years) the regolith has been mixed down to a depth of about one meter through the gardening effect (Neukum, Ivanov 1994). Then 2 g/cm^2 sulfur content corresponds to about 1 wt % in 1 m top layer of the regolith. If there are effective mechanisms of sulfur loss from cold traps, the sulfur abundance should be less than that of iron sulfide.

5. Detection of lunar polar volatiles by gamma-ray spectroscopy

Gamma-ray, infrared and optical spectrometers onboard future lunar polar missions

would determine the presence of lunar polar volatiles. The SELENE project is a Japanese lunar polar orbiter scheduled to be launched in 2005. This spacecraft will study the Moon for one year at an altitude of about 100 km. A Ge detector with an excellent energy resolution (~ 3 keV at 1.33 MeV) will be carried on SELENE as a gamma-ray detector for the first time in lunar gamma-ray spectroscopy (Hasebe et al. 1999). In the following, we estimate the possibilities of H, S, and C detection in the polar regions. The SELENE gamma-ray spectrometer collects 5 and 80 hours/year*resolution element at 60 degrees of latitude and at the poles, respectively (Hasebe et al. 1999). The most intensive carbon line at 4.438 MeV is difficult to detect because of interference from the strong O line of the same energy. Other C lines at 1.262, 3.684, and 4.945 MeV are also very close to strong O lines. So carbon on the Moon is practically difficult to detect using gamma-ray spectroscopic techniques. The first year observations by SELENE will collect data from the regions stable for sulfur for 400 hours. Major gamma-ray lines emitted from sulfur through neutron capture and inelastic scattering reactions are 0.841, 2.230, 2.380, 3.221, and 5.421 MeV. The intense line at 0.841 MeV lies at a distance of only 3 keV from a strong Al line. The intense line at 5.421 MeV is free from interference with surrounding lines of other elements. Ten hours of accumulation by a lunar polar mission carrying a Ge gamma-ray detector, for instance, enables one to detect more than 0.5 wt % S and 0.06 wt % H in

lunar soil (Metzger, Drake 1990). SELENE GRS can clearly identify the most intense hydrogen line at 2.2233 MeV. For 40 hours of integration, it will be possible to measure 0.1 wt % H (Kobayashi et al. 2002).

We have made Monte Carlo simulations for gamma-ray spectra expected for lunar polar regolith containing different H and S abundances. In these simulations, the Geant4 code was used. Computer simulations were made taking consideration of reducing the continuum Compton backgrounds and escape lines by the BGO anticoincidence system for Ge detector, but without considering Compton scattering for gamma-ray photons in the lunar regolith, and without considering the background produced in the spacecraft body. So the real background counting rate may be higher than that obtained in the simulations. The broadening of gamma-ray lines is also not considered. The chemical composition of dry regolith used in calculations is the following: O - 43.5, Si - 20, Al - 11, Ca - 10, Fe - 9, Mg - 4, Ti - 1.4, Na – 0.35, S - 0.07 wt %, K - 1200, H - 50, Th - 1.9, U - 0.5 ppm. If the energy resolution for the Ge detector is less than 5 keV at 2.2 MeV, a weak hydrogen line at 2.2233 MeV and a sulfur line at 2.230 MeV can be resolved near the strong Al line at 2.2104 MeV and Si line at 2.2354 MeV. The sulfur lines at 2.3797 and 2.230 MeV and the hydrogen line at 2.223 MeV cannot be seen in the case of observations for dry regolith over an 80-hour counting interval (see figure 6). Let us note that the anticoincidence system can

significantly decrease the background level and intensity of escape peaks. Using these assumptions it is possible to detect volatile elements over 80 hours of accumulation, if the H and S contents are higher than 0.02 and 0.3 wt %, respectively (see figure 7). The Ge spectrometer will collect about 40 photons of hydrogen and 100 photons of sulfur at the background level of 70 and 150 counts/keV, respectively. The width of the Al peak at 2210 keV is 10 keV due to the broadening effect; it will give an additional 10-20 photons to the background at the position of the hydrogen line in comparison with the results of calculations shown on figure 7. Simulations considering Compton scattering in the lunar regolith and the anticoincidence mode give a background level equal to 600 counts/keV*80 hours at 2.2 MeV. This means that the sensitivity of SELENE GRS will be three times lower than that shown on figures 6 - 8. So by 80 hours of accumulation, it is possible to detect hydrogen and sulfur, if their contents are higher than 0.05 and 1 wt %, respectively. Our lower limits to detect H and S contents are higher than those given by Metzger, Drake (1990). Let us note that the mean hydrogen content at for the SELENE GRS spatial resolution equal to 130 km is 0.01 –0.02 wt % near the poles (Feldman et al. 2001). Therefore, the SELENE gamma-ray spectrometer can confirm the results of the Lunar Prospector neutron spectrometer that hydrogen exists near the poles of the Moon only for a long counting interval (300-500 hours). Such long counting times can be achieved for regions poleward of 80 degrees in the first year of

observations. So the threshold of hydrogen content detectable for the SELENE gamma-ray spectrometer is significantly higher than that for the Lunar Prospector neutron spectrometer.

Let us check the detection possibility of SO_2 ice at the lunar poles by gamma-ray spectroscopy. Rough estimates based on the area with thermal stability for ice and its content (1500 km^2 and 2 wt %, see section 3 in this article) show that the sulfur content may be enhanced by 50-200 ppm over a 130 km polar lunar region (which is the SELENE GRS spatial resolution) due to the presence of SO_2 ice. However, this is too low in content for gamma-ray spectroscopy to detect it. The presence of SO_2 and CO_2 ices will be established by the in-situ chemical analysis of lunar polar samples or after returning them to the Earth.

Recently Hodges (2002b) proposed that the presence of unusual minerals with very low Ca or Si content in dry regolith instead of wet regolith could explain the decrease of epithermal neutron flux over the lunar poles. The SELENE gamma-ray spectrometer can check this hypothesis of unusual chemical composition at the poles. This instrument can measure abundances of Ca, Mg, Si, Fe, O, Ti, Th, Al, K and U with better accuracy than the Lunar Prospector gamma-ray spectrometer due to better energy resolution. For example simulations considering Compton scattering in the lunar regolith and anticoincidence mode give a background level equal to 40 counts/keV*13

hours near Ca lines at 3736 and 3904 keV. It will be possible to determine the Ca content with an accuracy of 30 % for 13 hours of accumulation time (see figure 8).

6. Concluding remarks

There are some restrictions on the cometary origin of lunar polar hydrogen. Large amounts of water are delivered to the polar regions only by large short-period comets. However, the characteristic time for collisions between active short-period comets with diameter of 5 km and the Moon is comparable with the age of the Solar system. Only if non-active short-period comets exist, the cometary origin of lunar hydrogen cannot be rejected. However, the population and the size distribution of non-active short-period comets are unknown. Future photometric and spectral observations of celestial bodies crossing the Earth's orbit are required for a better understanding of relationships between active comets, non-active comets, and asteroids.

The presence of CO_2 and SO_2 ices in the subsurface and at the surface is very sensitive to the temperature in polar traps. In principle, their ices of cometary origin could be stable at the surface of the coldest parts of permanently shadowed regions, but further processes retaining these ices should be studied. For an accurate determination of the area where CO_2 and SO_2 are stable, the temperature range in the lunar polar craters should be investigated in detail. One of most important problems for the

determination of subsurface temperature in polar traps is whether there exists a top 2 cm layer with extremely low heat conductivity at the poles or not. Measurements of brightness temperature at 0.1 mm – 3 cm and thermal neutron spectroscopy onboard future lunar polar satellites will make clear the existence of this unique layer.

The sulfur content deposited over a total area of about 10^{15} cm^2 near the lunar poles is estimated to be as high as 1 wt % if the delivery rate of sulfur is significantly higher than the loss rate. Future polar lunar missions should determine the composition and spatial distribution of volatiles. The Ge gamma-ray spectrometer onboard SELENE mission, for example, will be able to detect sulfur and hydrogen at the lunar poles if their content is higher than 1 and 0.05 wt %, respectively. However, in order to solve the question of their origin, we should wait for lunar polar rovers or penetrators carrying gamma-ray and mass-spectrometers.

Acknowledgments A.A. Berezhnoy is supported by a postdoctoral fellowship grant (No. P02059) from the Japanese Society for the Promotion of Science (JSPS). The authors wish to thank T. Mukai for useful comments and suggestions.

References

Ahrens, T.J., & O'Keefe, J.D. 1977, Impact and explosion cratering (New York: Pergamon Press)

Arnold, J.R. 1979, J. Geophys. Res., 84, 5659

Baulch, D.L., Duxbury, J., & Grant, S.J. 1976, Evaluated kinetic data for high temperature reactions: Homogeneous gas phase reactions of the O_2 - O_3 system, the CO - O_2 - H_2 system, and of sulphur-containing compounds, V. 3 (London–Boston: Butterworth)

Berezhnoi, A.A., & Klumov, B.A. 1998, JETP Lett., 68, 163

Berezhnoi, A.A., & Klumov, B.A. 2000, in Proceedings of the 4th International Conference on Exploration and Utilization of the Moon, ed. B.H. Foing & M. Perry, 175

Butler, B.J. 1997, J. Geophys. Res., 102, 19283

Cocks, F.H., Klenk, P.A., Watkins, S.A., Simmons, W.N., Cocks, J.C., Cocks, E.E., & Sussingham, J.C. 2002, Icarus, 160, 386

Crider, D.H., & Vondrak, R.R. 2000, J. Geophys. Res., 105, 26773

Delsemme, A.H. 1988, Royal Soc. Philos. Transact., Ser. A, 325, 509

Donnison, J.R. 1986, A&A, 167, 359

Duxbury, N.S., Nealson, K.H., & Romanovsky, V.E. 2001, J. Geophys. Res., 106, 27811

Fanale, F.P., & Salvail, J.R. 1989, Geophys. Res. Lett., 16, 287

Feldman, W.C., Maurice, S., Binder, A.B., Barraclough, B.L., Elphic, R.C., & Lawrence, D.J. 1998, Science, 281, 1496

Feldman, W.C., Lawrence, D.J., Elphic, R.C., Barraclough, B.L., Maurice, S., Genetay, I., & Binder, A.B. 2000, J. Geophys. Res., 105, 4175

Feldman, W. C., et al. 2001, J. Geophys. Res., 106, 23231

Hale, A.S., & Hapke, B. 2002, Icarus, 156, 318

Hasebe, N., et al. 1999, Adv. Space Res., 23, 1837

Hodges, R.R. 2002a, J. Geophys. Res., 107, E2, 6-1, CiteID 5011, DOI 10.1029/2000JE001491

Hodges, R.R. 2002b, J. Geophys. Res., 107, E12, 8-1, CiteID 5125, DOI 10.1029/2000JE001483

Hobbs, P.V. 1974, Ice physics (Oxford: Clarendon Press)

Huebner, W.F., Keady, J.J., & Lyon, S.P. 1992, Astroph. Space Sc., 195, 1

Jeffers, S.V., Manley, S.P., Bailey, M.E., & Asher, D.J. 2001, MNRAS, 327, 126

Killen, R.M., Benkhoff, J., & Morgan T.H. 1997, Icarus, 125, 195

Klumov, B.A., & Berezhnoi, A.A. 2002, Adv. Space Res., 30, 1875

Kobayashi, M.N., et al. 2002 Adv. Space Res., 30, 1927

Langseth, M.G., Keihm, S.J., & Peters, K. 1976, in Proceedings of 7th Lunar Science Conference, V. 3 (New York: Pergamon Press), 3143

Lanzerotti, L.J., Brown, W.L., & Johnson, R.E. 1981, J. Geophys. Res., 86, 3949

Lauretta, D.S., Kremser, D.T., & Fegley, Br.Jr. 1996, Icarus, 122, 288

Le Teuff, Y. H., Millar, T. J., & Markwick, A. J. 2000, A&AS, 146, 157

Love, S. G., Brownlee, D. E. 1993, Science, 262, 550

Margot, J.L., Campbell, D.B., Jurgens, R.F., & Slade, M.A. 1999, Science, 284, 1658

Mellon, M.T., Jakosky, B.M., & Postawko, S.E. 1997, J. Geophys. Res., 102, 19357

Metzger, A.E., & Drake, D.M. 1990, J. Geophys. Res., 95, 449

Moore, C.B., Lewis, C.F., & Cripe, J.D. 1974, in Proceedings of 5th Lunar Science Conference, V. 2 (New York: Pergamon Press), 1897

Morgan, T.H., & Shemansky, D.E. 1991, J. Geophys. Res., 96, 1351

Moses, J.I., Rawlins, K., Zahnle, K., & Dones, L. 1999, Icarus, 137, 197

Neukum, G., & Ivanov, B.A. 1994, in Hazards due to comets and asteroids, ed. T. Gehrels, M.S. Matthews, & A. Schumann (Tucson: University of Arizona Press), 359

Nimmo, W., Hampartsoumian, E., Hughes, K.J., & Tomlin, A.S. 1998, in Proceedings of 27th International Symposium on Combustion, 1, 1419

Nozette, S., Lichtenberg, C.L., Spudis, P.D., Bonner, R., Ort, W., Malaret, E., Robinson, M., & Shoemaker, E.M. 1996, Science, 275, 1495

Nozette, S., Spudis, P.D., Robinson, M.S., Bussey, D.B., Lichtenberg, C.L., & Bonner, R. 2001, J. Geophys. Res., 106, 23253

Rabinowitz, D. L., Bowell, E., Shoemaker, E. M., & Muinonen, K. 1994, in Hazards due to

comets and asteroids, ed. T. Gehrels, M.S. Matthews, & A. Schumann (Tucson: University of Arizona Press), 285

Shafer, C.M., Gloeckler, G., Galvin, A. B., Ipavich, F.M., Geiss, J., von Steiger, R., & Ogilvie, K. 1993, Adv. Sp. Res., 13, 79

Shoemaker, E.M., Weissmann, P.R., & Shoemaker, C.S. 1994, in Hazards due to comets and asteroids, ed. T. Gehrels, M.S. Matthews, & A. Schumann (Tucson: University of Arizona Press), 313

Sprague, A. L., Hunten, D. M., & Lodders, K. 1995, Icarus, 118, 211

Starukhina, L.V., & Shkuratov, Y.G. 2000, Icarus, 147, 585

Vaniman, D., Pettit, D., & Heiken, G. 1992, in Proceedings of the Second Conference on Lunar Bases and Space Activities of the 21st Century, ed. W.W. Mendell (Washington: NASA Conf. Pub.), V. 2, 429

Vasavada, A.R., Paige, D.A., & Wood, S.E. 1999, Icarus, 141, 179

Vondrak R.R. 1974, Nature, 248, 657

Watson, K., Murray, B.C., & Brown, H. J. 1961, J. Geophys. Res., 66, 3033

Werner, S. C., Harris, A. W., Neukum, G., Ivanov, B. A. 2002, Icarus, 156, 287

Zel’dovich, Y.B., & Raizer, Y.P. 1967, Physics of Shock Waves and High-Temperature Hydrodynamic Phenomena, ed. W.D. Hayes & R.F. Probstein, V. II (New York: Academic Press)

Compound	M_r, g/mole	t_{ph}, s	K
CO_2	44	$5*10^5$	0.01
H_2O	18	$8*10^4$	0.04
SO_2	64	$5*10^3$	0.001
H_2S	34	$3*10^3$	0.0001
S	32	10^6	1

Table 1. The capture probability of gases from the lunar exosphere by cold traps.

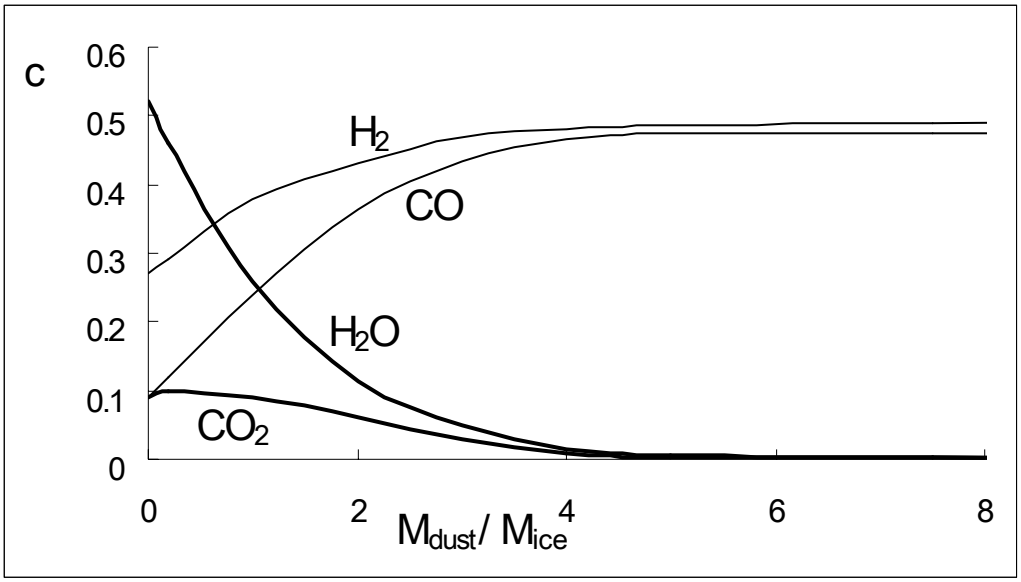

Fig. 1. Equilibrium chemical composition of impact-produced fireball at 1300 K and 0.001 bar versus dust/gas ratio in cometary matter. The elemental compositions of cometary dust and gas components are taken to be equal to those of comet Halley (Delsemme 1988).

Fig. 2. The chemical composition of impact-produced lunar atmosphere versus time. The gas temperature is 300 K; the initial number density is 10^{13} cm^{-3}. The initial abundances of species are equal to the equilibrium abundances in the fireball at 1700 K and 1 bar. The fireball is formed after the collision of a C-rich comet with the Moon.

Fig. 3. The chemical composition of impact-produced lunar atmosphere versus time. The gas temperature is 300 K, the initial number density is 10^{13} cm^{-3}. The initial abundances of species are equal to the equilibrium abundances in the fireball at 700 K and 0.01 bar. The fireball is formed after the collision of an O-rich comet with the Moon.

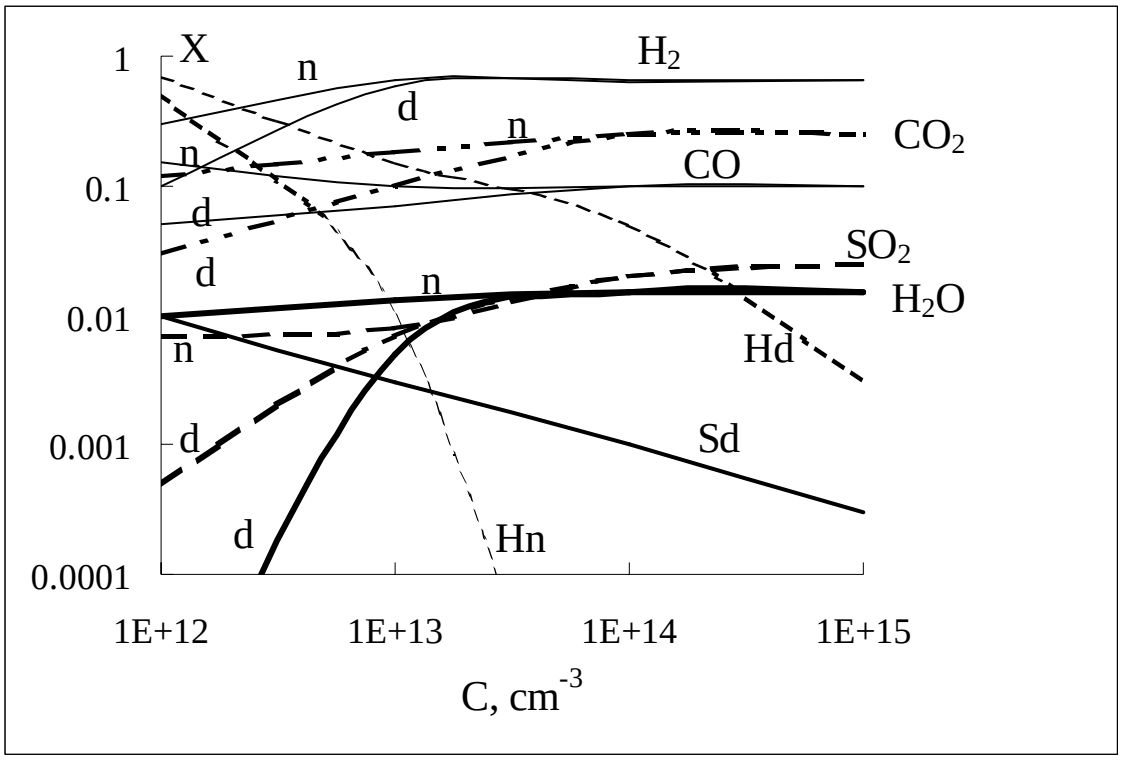

Fig. 4. The quasi-equilibrium chemical composition of temporary lunar atmosphere versus total number density. The gas temperature is 300 K. The initial abundances of species are equal to the equilibrium abundances in the fireball at 1700 K and 1 bar. The fireball is formed by the collision of an O-rich comet with the Moon. The symbols “d” and “n” indicate the daytime and nighttime abundances, respectively.

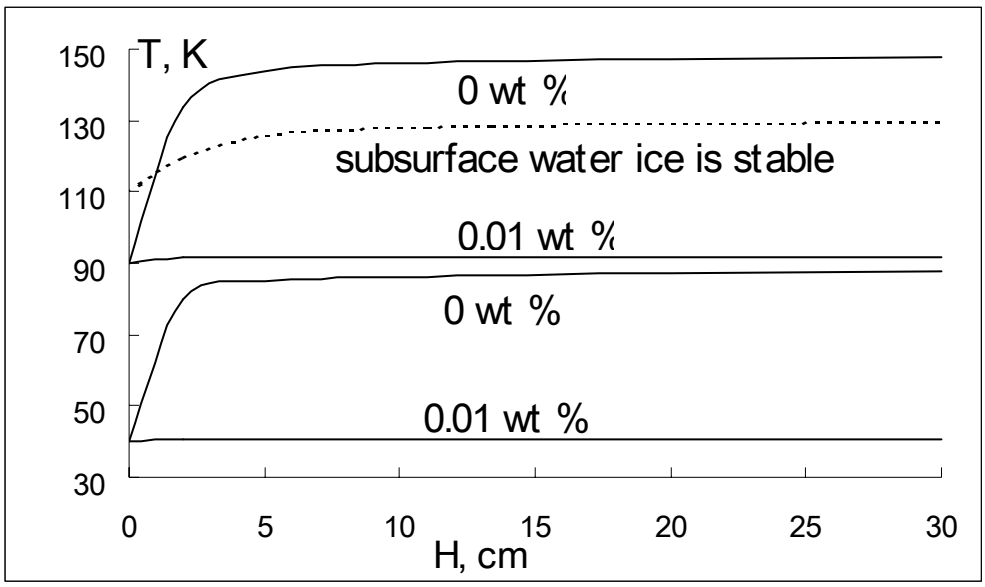

Fig. 5. Mean regolith temperature in lunar cold traps versus the depth H at different surface average temperatures (40 and 90 K) and water ice content (0 and 0.01 wt %). The dashed line shows the dependence of the average regolith temperature on the depth; under these conditions the lunar polar regolith with 1 wt % water ice all the water ice will have disappeared by sublimation after one billion years.

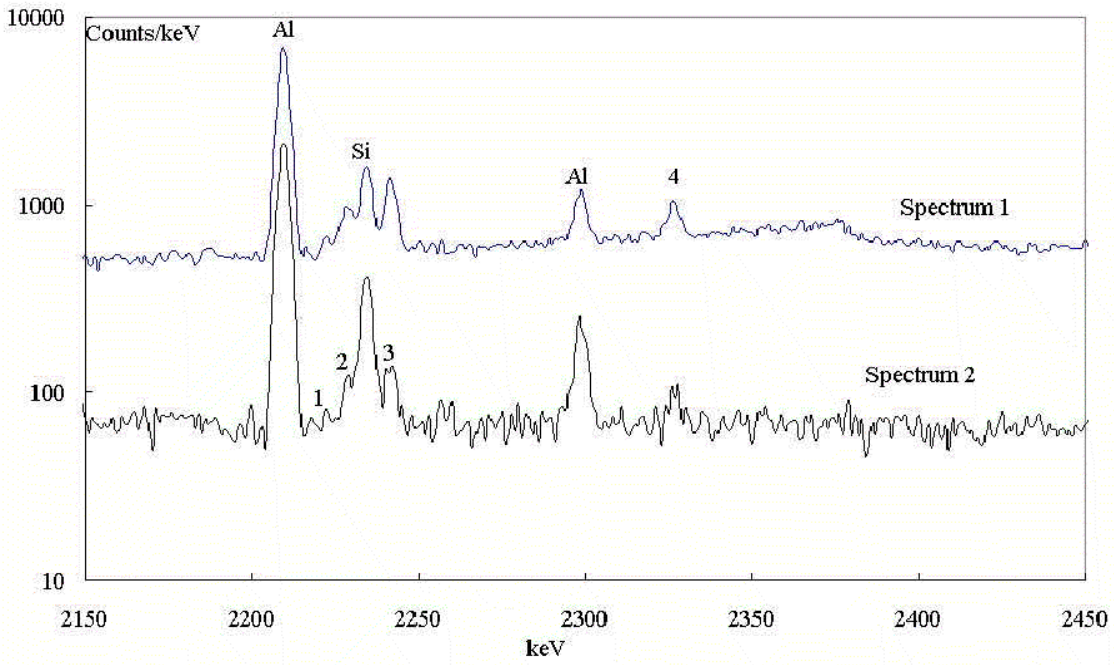

Fig. 6. Expected energy spectra from the lunar surface obtained by SELENE gamma-ray spectrometer. Number 1 – H line, 2 - O single escape peak, 3 – Mg, Al, Si escape peaks. 4 - Si single escape peak. The accumulation time is 80 hours. The hydrogen and sulfur contents are equal to 0.005 and 0.07 wt % respectively. Spectrum 1 is calculated without anticoincidence mode, spectrum 2 is calculated with BGO anticoincidence mode against the Ge detector. The spectra are calculated neglecting Compton scattering in the lunar regolith.

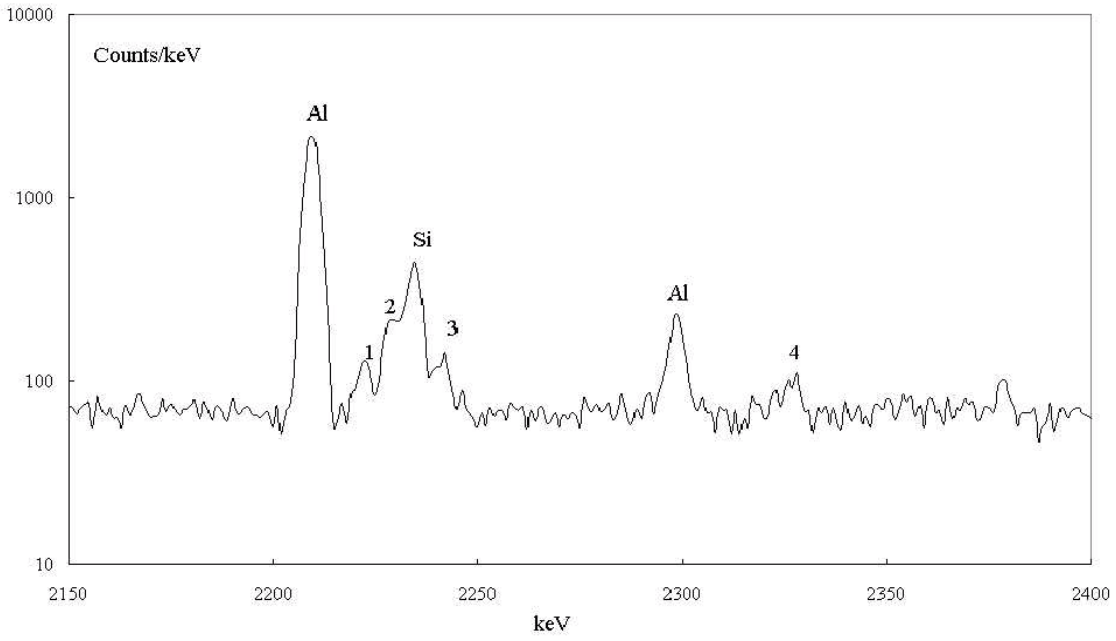

Fig. 7. Expected energy spectrum from the lunar surface obtained by SELENE gamma-ray spectrometer. Number 1 – H line, 2 – S line and O single escape peak, 3 – Mg, Al, Si escape peaks, 4 - Si single escape peak. The accumulation time is 80 hours. The hydrogen and sulfur contents are equal to 0.02 and 0.5 wt % respectively. The spectrum is calculated with BGO anticoincidence mode against the Ge detector and neglecting Compton scattering in the lunar regolith.

Fig 8. Expected energy spectrum for 3 - 4 MeV range from the lunar surface obtained by SELENE gamma-ray spectrometer. The accumulation time is 13 hours. The spectrum is calculated without BGO anticoincidence mode against the Ge detector and neglecting Compton scattering in the lunar regolith.